Potential Active Shooter Detection Based on Radar Micro-Doppler and Range-Doppler Analysis Using Artificial Neural Network

Yiran Li, *Student Member, IEEE*, Zhengyu Peng, *Student Member, IEEE*, Ranadip Pal, *Senior Member, IEEE*, and Changzhi Li, *Senior Member, IEEE*

***Abstract*— This paper presents a detection method of remotely identifying a potential active shooter with a concealed rifle/shotgun based on radar micro-Doppler and range-Doppler signature analysis. By studying and comparing the micro-Doppler and range-Doppler information of human subjects carrying a concealed rifle versus other similar activities, special features are extracted and applied for detecting people with suspicious behaviors. An artificial neural network is adopted in this work to complete the activity classification, and the classification result shows a 99.21% accuracy of differentiating human subjects carrying a concealed rifle from other similar activities. Due to the properties of radar sensor, the proposed method does not involve sensitive information such as visual images, and thus can better protect the privacy while being able to see-through the clothing for reliable detection.**

***Index Terms*— Active shooter detection, micro-Doppler, range-Doppler, radar sensors, artificial neural network.**

I. Introduction

THE number of active shooting incidents rises year by year in many countries over the world. The latest Federal Bureau of Investigation (FBI) report shows that the number of active shooting incidents in the 2014-2015 period is six times as high as the number of incidents during the 2000-2001 period. Among the incidents that occurred during the 2014-2015 period, 40% of the incidents had shotguns or rifles involved and caused 57% of total killed casualties [1]. Current technologies on market for shooter detection include acoustic gunshot identification and infrared camera gunfire flash detection [2]. However, both technologies only trigger an alarm after a weapon is fired. Although current systems could speed up the police's response time, they do not prevent those incidents from happening. Thus, an effective shooter detection system, especially for detecting shooters armed with concealed rifle/shotgun before the shooter draws the weapon, is highly demanded to prevent such tragedies.

Manuscript received September 14, 2018; revised October 21, 2018; accepted October 26, 2018. Date of publication November 1, 2018; date of current version January 11, 2019. This work was supported by NSF under Grant ECCS-1808613 and Grant CNS-1718483. The associate editor coordinating the review of this paper and approving it for publication was Dr. Ioannis Raptis. *(Corresponding author: Yiran Li.)*

Y. Li, R. Pal, and C. Li are with the Department of Electrical and Computer Engineering, Texas Tech University, Lubbock, TX 79409 USA (e-mail: yiran.li@ttu.edu; ranadip.pal@ttu.edu; changzhi.li@ttu.edu).

Z. Peng was with the Department of Electrical and Computer Engineering, Texas Tech University, Lubbock, TX 79409 USA. He is now with Aptiv, Kokomo, IN 46903 USA (e-mail: zpeng.me@gmail.com).

Digital Object Identifier 10.1109/JSEN.2018.2879223

In the meantime, radar-measured micro-Doppler signature provides useful information related to moving objects and has been widely studied for targets and activities recognition and classification. Many works have shown the possibility to use micro-Doppler signature analysis into activity classification [3], [4], target recognition [5]–[7], healthcare applications [8]–[10] and smart home applications [11], [12].

Quite a few works showed the feasibility of applying micro-Doppler signature processing in security applications. For example, [5] used micro-Doppler to characterize and differentiate humans, animals and vehicles. Reference [13] pointed out the potential to estimate human motion and determine if the human subject is carrying a weapon based on the micro-Doppler signature caused by arm motion. Fioranelli *et al.* [14] used a multistatic radar system to distinguish unarmed and potentially armed personnel. Both [13] and [14] focused on the analysis of micro-Doppler caused by arm motion and a metallic pole representing a rifle was used in [14] for their experiments.

Other than micro-Doppler signature, range-Doppler signature is another type of radar signature. It tracks the range profile of a walking person by measuring the distance between the person and the device. It also provides velocity information of a moving target. Thus, range-Doppler signature is very useful for tracking and locating a moving target and could serve as a great supplement to the conventional micro-Doppler analysis for gait and gesture classification. References [15]–[17] studied combining multiple domain analysis for fall detection. Integrated slow-time range-Doppler map [15] and range-map [15]–[17] were utilized in the research. The classification results from [15]–[17] showed the classification rate can be improved by combining information from multiple domains.

Various methods of feature extraction and recognition for activity classification were presented in different works. The key purpose of feature extraction is to obtain the most distinguishable features of different activities. Principal component analysis (PCA) was adopted in [12], [18], and [19]. Singular value decomposition (SVD) was employed in [20]. For activity recognition, References [3] and [4] used support vector machine (SVM) and artificial neural network (ANN), respectively, to realize human activity classification. Reference [11] adopted convolutional neural network (CNN) as the classifier.

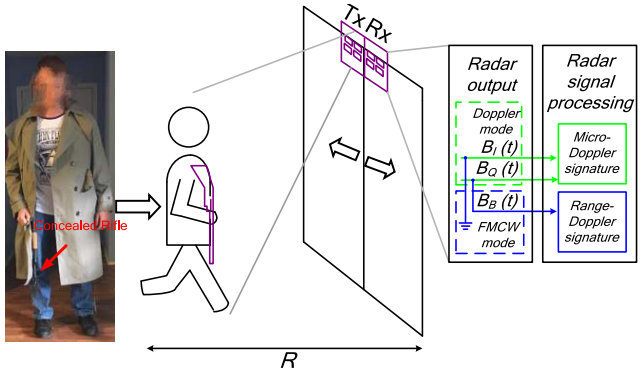

Fig. 1. Application scenario of the proposed active shooter detection system.

The proposed work investigates the potential of using portable radar sensors for active shooter detection by analyzing both micro-Doppler and range-Doppler signatures. It aims to recognize a shooter with a concealed rifle/shotgun before the weapon is drawn. The proposed method realizes the detection by identifying special gaits and gesture characteristics of a person walking with a concealed rifle. The patterns produced by a human body and a concealed weapon on radar signatures are analyzed. To the best of authors' knowledge, using concurrent micro-Doppler and range-Doppler signature analyses for potential active shooter detection has never been studied. Furthermore, radar signatures of seven other activities in the same application scenario are studied and compared with signatures corresponding to a person walking with a concealed rifle. Thirteen human subjects are used in the experiments to collect over 4000 samples. An ANN is adopted for activity classification based on five features extracted. The capability of the proposed method for recognizing movements from different angles and under different noise levels is studied.

This paper is organized as follows. The micro-Doppler and range-Doppler signatures obtained by radar sensor are illustrated in Section II. Radar hardware, experiments and results for different activities are described in Section III. In Section IV, feature extraction and activity classification are presented. A conclusion is drawn in Section V.

II. Micro-Doppler and Range-Doppler

Micro-Doppler and range-Doppler are two special features obtained from radar output when radar operates under the Doppler mode and the frequency-modulated continues-wave (FMCW) mode, respectively. Fig. 1 shows one of the application scenarios of the proposed potential active shooter detection system. A radar sensor is mounted at the entrance of a building or a monitored area inside a building. A potential active shooter carrying a rifle is walking toward the door at distance R. The radar transmitted signal is reflected by the moving target and the reflected signal is received and processed by the radar receiver (Rx) end. Two radar output channels are sampled and collected as the I and Q channel radar outputs $B_I(t)$ and $B_Q(t)$ when the radar works under Doppler mode. One output channel is grounded and the other output channel is sampled and collected as the beat signal $B_B(t)$ while the radar operates under FMCW mode.

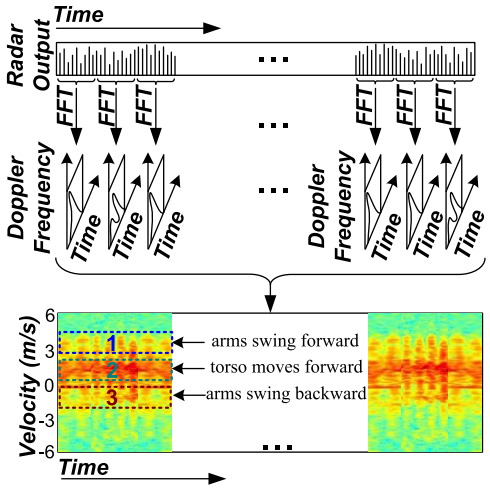

Fig. 2. Process to obtain micro-Doppler signature from radar output.

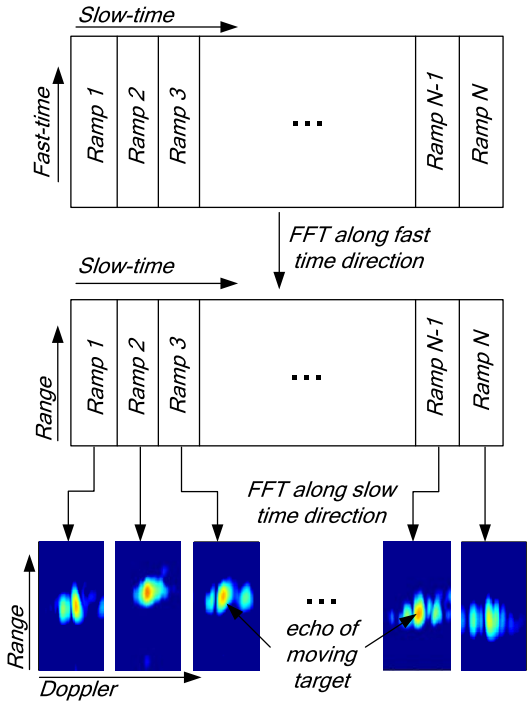

Fig. 3. Process to obtain range-Doppler signature from radar output.

Micro-Doppler and range-Doppler signatures are created by processing those radar outputs. Figs. 2 and 3 illustrate the process of deriving those two signatures from the radar output.

A. Micro-Doppler Signature

As shown in Fig. 1, when the radar sensor operates under the Doppler mode, radar output signals $B_I(t)$ and $B_Q(t)$ are collected. Those two signals can be expressed as:

$$B_I(t) = A_I \cdot \cos(2\pi \cdot f_D \cdot t + \Delta\phi) \quad (1)$$

$$B_Q(t) = A_Q \cdot \sin(2\pi \cdot f_D \cdot t + \Delta\phi) \quad (2)$$

where A_I and A_Q are the amplitudes of the I and Q channel, respectively, $\Delta\phi$ is related to the phase shift of propagation and phase noise of the system. f_D is the term representing Doppler frequency shift. Furthermore, due to the relationship

between the Doppler frequency shift and actual movement velocity, the speed of the moving target can be calculated as:

$$v_{\text{object}} = \frac{c \times f_D}{2 \times f_T} \tag{3}$$

where f_{T} is the radar carrier frequency, and c is the speed of light.

Micro-Doppler signature is created by applying Short-Time Fourier Transform (STFT) to radar output. Fig. 2 shows the process of obtaining micro-Doppler signature from the radar output. The sampled radar output is a series of voltage readings that form a one-dimensional array along time. As shown in Fig. 2, to perform STFT, the radar output is divided into short segments with equal length. Fast Fourier Transform (FFT) is taken for each segment and the Doppler shift due to the movement of the target is revealed for each short period. Usually, STFT result is derived by combining each FFT result and showing the spectra changes over time. The bottom plot in Fig. 2 is an example of micro-Doppler signature obtained from the radar output.

Micro-Doppler signature provides useful velocity information related to different parts of a human body. For example, the bottom part of Fig. 2 shows the micro-Doppler signature for a human subject walking toward the radar sensor. The y-axis of this plot is the velocity converted from Doppler frequency shift based on (3). As labeled in the figure, the high power density area in region 1 represents arms swinging toward the radar sensor. Region 2 represents the torso moving toward the radar. Region 3 with a negative velocity corresponds to the moment when arms swing away from the radar.

B. Range-Doppler Signature

Range-Doppler contains range and velocity information of a moving target. As shown in Fig. 1, range-Doppler signature is derived from the beat signal $B_B(t)$ output from radar sensor when the radar works in the FMCW mode. The beat signal received from a stationary target can be expressed as [21], [22]:

$$B_B(t) = S_{Tx}(t) * S_{Rx}(t) = A_b \cdot exp(j \cdot 2\pi \cdot f_R \cdot t) \tag{4}$$

where $B_B(t)$ is the beat signal output from the radar configured in FMCW mode, $S_{Tx}(t)$ is the radar transmitted signal and $S_{Rx}(t)$ is the received signal. Complex amplitude A_b contains all the phase information. The f_R is the frequency difference between the received signal and a local copy of the transmitted signal and is linearly proportional to the target range R. Thus, the range information can be derived by applying FFT to the beat signal in (4).

When using FMCW radar to detect a moving target, the frequency of the received signal not only contains a frequency shift related to range information, but also has a frequency component corresponding to the Doppler shift. The beat signal in this case can be expressed as [21]:

$$B_B(t, t_i) = A_b \cdot exp(j \cdot (2\pi \cdot f_R \cdot t + 2\pi \cdot f_D \cdot t_i)) \tag{5}$$

where f_D is the term related to the target's velocity and can be obtained by applying another FFT of the beat signal.

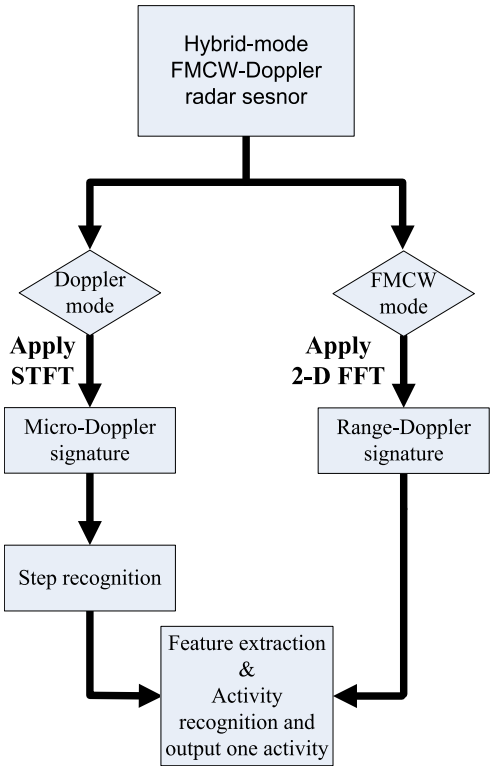

Fig. 4. Flow chart of the proposed potential active shooter detection method.

Thus, by applying 2-D FFT to the beat signal described in (5), both range and velocity information of a moving target can be revealed.

Figure 3 depicts the process of obtaining a range-Doppler image from the beat signal [21]. As shown in the top plot in Fig. 3, the sampled beat signal $B_B(t,\ t_i)$ is arranged as a two-dimensional array. Each column of the array is the sampled time-domain beat signal corresponding to one FMCW radar frequency ramp. In this array, the column-wise axis is related to the FMCW radar chirp repetition time and usually referred as "slow-time" while the row-wise axis is related to the sampling rate of beat signal and referred as "fast-time". Both the "slow-time" and "fast-time" directions are labeled in the top plot of Fig. 3.

As shown in the middle plot of Fig. 3, the range profile is revealed by taking FFT along the "fast-time" direction. Then, another FFT is taken along the "slow-time" direction to obtain the velocity information. The 2-D FFT operation result in a range-Doppler graph for the given time duration as shown at the bottom of Fig. 3. Similar to the micro-Doppler plot, the range-Doppler plot is a 2-D intensity image. The moving target forms a high energy echo on the range-Doppler plot. A few echoes produced by the moving target are labeled on the image at the bottom of Fig. 3. Both the range and velocity information of the moving target are simultaneously revealed. Thus, this type of radar signature can be adopted in potential active shooter detection to track the target of interest.

III. Experiment and Results

Figure 4 shows the flow chart of the proposed potential active shooter detection system. As shown in the flow chart,

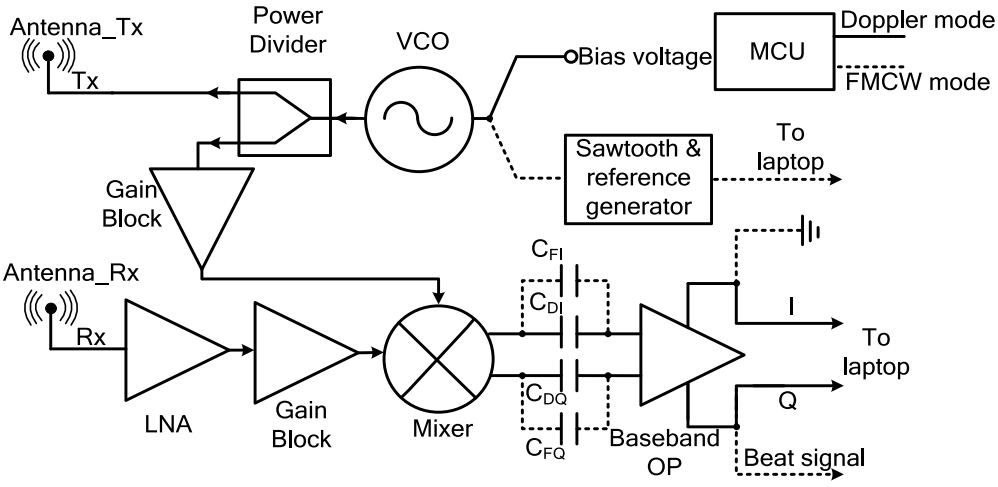

Fig. 5. Block diagram of the 5.8GHz hybrid-mode radar sensor.

a hybrid-mode FMCW-Doppler radar sensor is adopted. Micro-Doppler and range-Doppler signatures are obtained from radar output using the method introduced in section II. Feature extraction is performed after creating those radar signatures. A step recognition process is needed before extracting features from micro-Doppler signature. Activity is classified based on the extracted features. The output is an activity recognized by the proposed system. In this section, radar hardware and radar signatures obtained from experiments are described and discussed. Step recognition, feature extraction, and activity classification are introduced in the next section.

The custom-designed 5.8-GHz hybrid-mode FMCW-Doppler radar sensor proposed in [24] is adopted in this work. Experiments are conducted, and different human subjects are used to perform several activities. Micro-Doppler and range-Doppler are created from radar output. In this section, radar hardware, experiment setup, and radar signatures for different activities are depicted in detail.

It is necessary to mention that some preliminary experiment results and discussion present in this section were published in the authors' previous work [25]. However, there are significant differences between [25] and this work. In [25], only one human subject was used and the conclusion was made based on the observations from micro-Doppler and range-Doppler of different activities. In this work, more human subjects are used, and a lot of samples are collected. The authors focus on feature extraction and activity classification based on micro-Doppler and range-Doppler signature analysis in this study.

A. Radar Hardware

The micro-Doppler and range-Doppler signatures used in this work are obtained from the output of a hybrid-mode FMCW-Doppler radar sensor [24]. Fig. 5 shows the block diagram of this radar. Switching between different modes is realized by analog switches configured by a microcontroller. In Fig. 5, the solid line shows the signal path of Doppler mode while the dashed line indicates the signal path of FMCW mode.

When the radar works under the Doppler mode, a free-running voltage controlled oscillator (VCO) is adopted to generate a 5.8-GHz transmit signal and drive the mixer in the receiver chain. A low-noise amplifier (LNA), a gain block, a mixer and a baseband amplifier form the receiver chain. Two capacitors (C_{DI} and C_{DQ}) are used to realize ac-coupling and block dc component of the I/Q signal. The I and Q signals are collected under this mode.

When the radar works under the FMCW mode, a sawtooth and reference generator is employed to produce a "sawtooth" voltage to control the VCO. In order to achieve coherent detection, the beat signal and the synchronization signal, which is locked to the "sawtooth" voltage signal, are collected and sampled simultaneously.

The radar sensor has a transmit power of 8 dBm with a center frequency at 5.8 GHz. The bandwidth of the transmit signal is 320 MHz and the frequency of the sawtooth ramp is 82 Hz when the radar sensor works under FMCW mode. This corresponds to a range resolution of 0.47 m and chirp repetition rate of 82 Hz. All the radar outputs are sampled by the audio card on computer.

It should be noted that based on the common range (20 Hz to 20000 Hz) of human hearing, the audio card cuts all information at low frequency and only process signal above 20 Hz. Fortunately, the frequency range of interest in this work is within the audio card process range.

B. Experiment Setup and Results

Experiments were conducted to demonstrate the feasibility of using micro-Doppler and range-Doppler signatures to identify a person walking with a concealed rifle/shotgun. In order to test the proposed method's capability to differentiate similar activities, eight activities were performed by human subjects. Those activities include: (a) walking with a concealed rifle under trench coat, (b) walking without holding anything, (c) walking with a cane for the blind, (d) walking with a gym bag, (e) walking with a laptop, (f) walking with a walker, (g) moving in a wheelchair, and (h) walking with a rolling suitcase. To make the experiments close to real case,

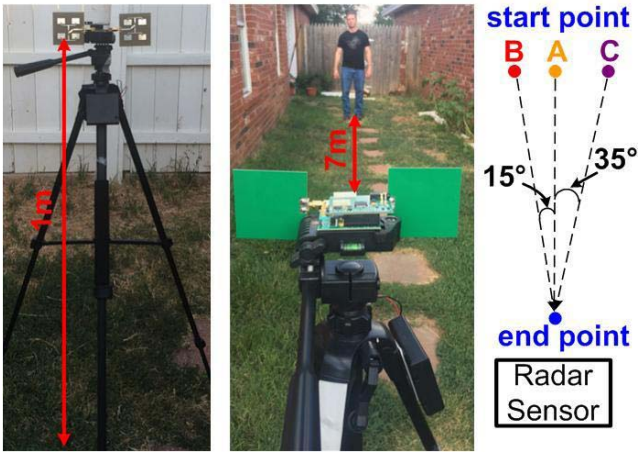

Fig. 6. Experiment setup.

activities selected in this study were chosen based on the author's observation from locations that the proposed technology could be applied to. Those locations include the entrances of a school, an airport, and a hospital.

The experiment setup is shown in Fig. 6. The tests were conducted outside and the radar sensor was fixed on a tripod at 1 meter above ground. A battery pack was mounted on the tripod to provide power to the radar system. A human subject was asked to start from point A in Fig. 6 and walk straight toward the radar. The start point A was seven meters away from the sensor. This movement had an angle of 0° to the radar antenna's main lobe. In this study, thirteen human subjects (ten males and three females) were used. Each human subject was asked to repeat every activity for four times. Furthermore, in order to test the recognition capability of the proposed method under different movement angles, two other start points (B and C) were adopted and the movements from those two points were 15° and 35° to the radar, respectively. Three human subjects were asked to perform each activity for 4 times starting from those two points.

Figure 7 shows an example of micro-Doppler (a) and range-Doppler (b) signatures obtained by the radar sensor working under different modes. A human subject was asked to walk toward the sensor without holding anything in this example. As mentioned in section II, micro-Doppler signatures are created by applying STFT to the radar output. In this work, a sliding window size of 1.024 second is used and the Hamming window is adopted. The velocity information regarding different body parts can be revealed on micro-Doppler signature. In Fig. 7(a), the subject walked eight steps toward the sensor, with one of the steps labeled in the figure. For each step, besides the torso movement, large positive and negative frequency shifts are generated by natural arm swings. The velocity can be derived from frequency shift based on (3). The velocity is labeled on the y-axis in Fig. 7(a) and the negative sign means the part of the target receded from the radar.

Fig. 7(b) is an example of a range-Doppler signature obtained at the moment when a human subject walked toward the radar without holding anything. The range and velocity

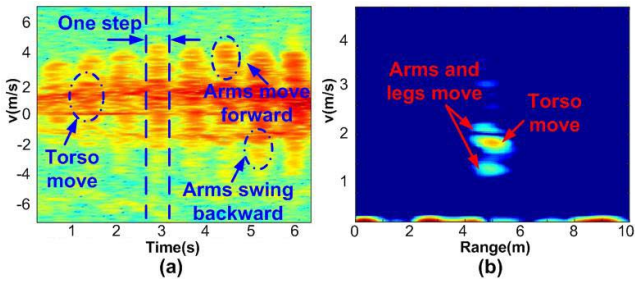

Fig. 7. An example of micro-Doppler (a) and range-Doppler (b) signatures obtained when a test subject walks naturally toward the radar sensor.

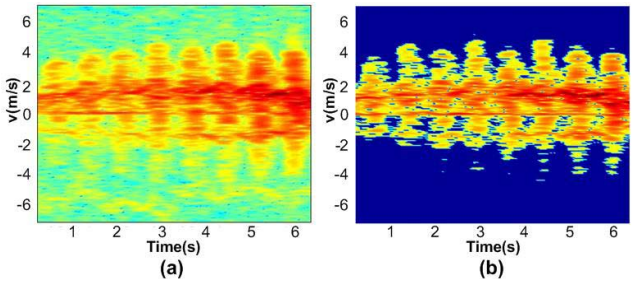

Fig. 8. Micro-Doppler signature of a human subject walks naturally toward the radar sensor (a) before and (b) after noise removal.

information can be read from the signature. Comparing the range-Doppler signature with the micro-Doppler signature in Fig. 7(a), the torso and limbs movement can be identified on the range-Doppler graph. For example, in the micro-Doppler signature, the torso movement has an average speed around 2 m/s. Thus, the human signature at around 2 m/s in range-Doppler signature corresponds to the torso movement of the subject. In addition, the range-Doppler provides the absolute distance between the radar sensor and the moving object, which is helpful for locating a potential shooter. It should be noticed that only positive Doppler frequency shift is plotted on this range-Doppler graph. This is because the human subject was always asked to walk toward the radar and the high intensity torso radar echo always shows up with positive Doppler frequency shift.

In order to effectively process radar signatures, a noise removal algorithm is applied after obtaining the micro-Doppler signature. Fig. 8 shows an example of micro-Doppler signatures before (a) and after (b) noise removal when a human subject walked toward radar sensor without holding anything. Fig. 8(a) is the original micro-Doppler derived from the radar output. A power density threshold is set and any value below the threshold is set to a very small value (-60 in this work). Fig. 8(b) is the micro-Doppler after noise removal. The information of the human subject movement is well preserved while the noise at undesired frequency is filtered out. It should be noted that the main sources of the noise in the experiments is small vibrations from the testing environment (e.g. radar device vibration due to the wind). In the real applications, the device will be firmly mounted at an indoor area or the area connecting indoor and outdoor. Thus, the noise from the environment would be less severe than that in the experiments.

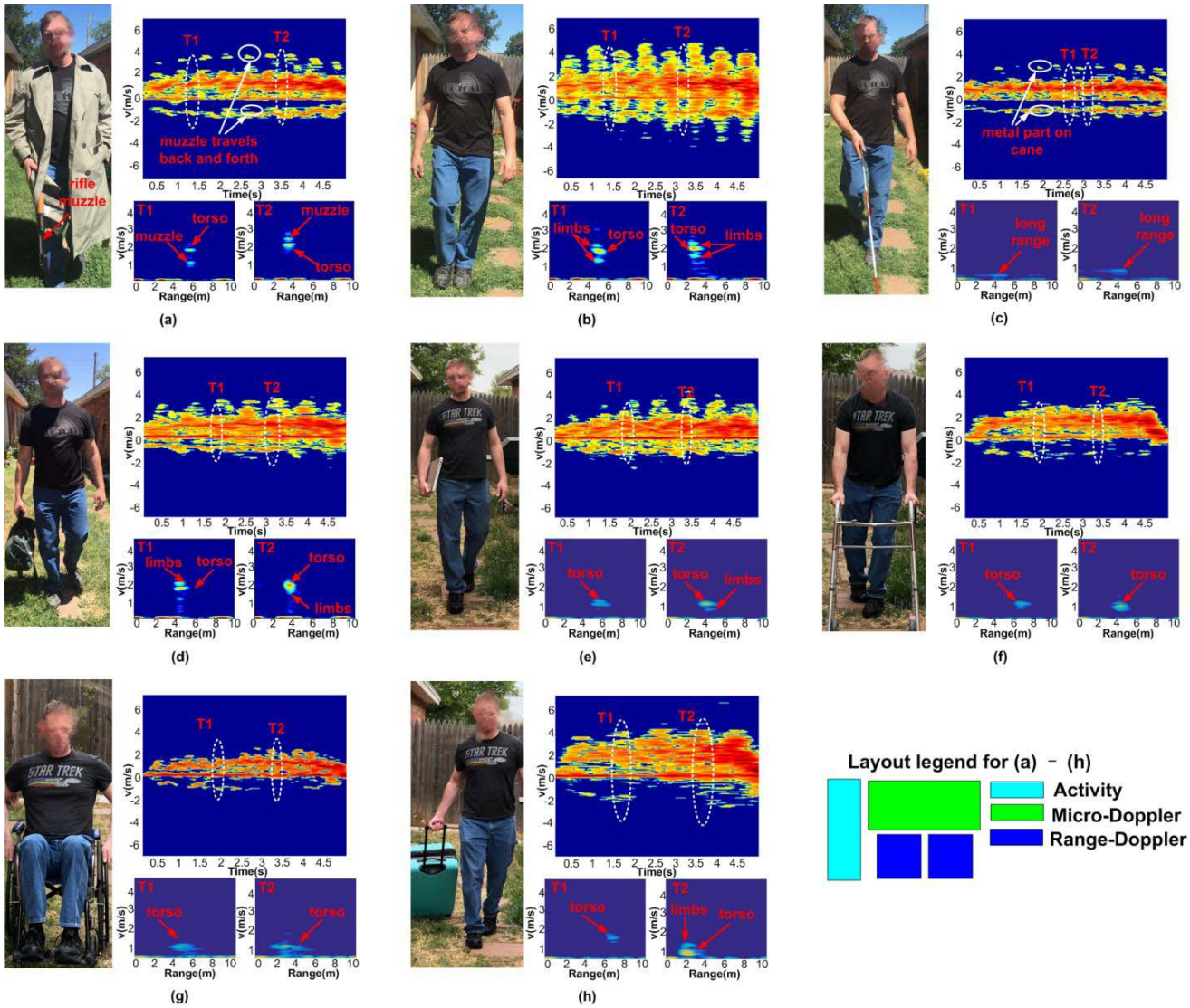

Fig. 9. Micro-Doppler and range-Doppler for different activities: (a) walking with a concealed rifle, (b) walking with natural arm swings, (c) walking with a cane for a blind person, (d) walking while holding a gym bag, (e) walking while carrying a laptop, (f) walking with a walker, (g) moving in a wheelchair, and (h) walking with a rolling suitcase.

Figure 9 shows the experiment results. Each sub-figure corresponds to one type of activities. In each sub-figure, a picture with a human subject presenting the activity is shown on the left. On the right, the micro-Doppler signature after noise removal is shown on top and two range-Doppler signatures obtained at two different moments (T_1 and T_2 as marked in the spectrogram) are placed on the bottom.

By studying and comparing the micro-Doppler and range-Doppler images obtained from each test, some special features were discovered and could be used to identify a potential shooter. The analysis for each case is discussed below [25]:

1) Walking With a Concealed Rifle Under Trench Coat : As shown in the micro-Doppler signature of Fig. 9(a), the person walked nine steps toward the radar. The power density of signal due to torso movement is high. However, since the rifle is usually long and heavy and the subject tried to hide it close to his/her body, the arm movement was very limited [25]. Thus, there is no large frequency shift for limbs shown on the signature. However, the metal parts on the gun, especially the tip of the gun (i.e., the muzzle) that traveled with the longest distance in each step, creates strong reflection and led to a high power density on the signature [25]. The move of the muzzle for one step is labeled in the figure.

The two range-Doppler signatures in Fig. 9(a) reveal the range information of the moving subject at moments T_1 and T_2. In each frame, the high density radar echo area at around 2 m/s corresponds to the torso movement. The radar echo around 1 m/s in the first frame and the echo around 2.5 m/s in the second frame represent the movement of the muzzle on the rifle.

2) Walking Without Holding Anything: The micro-Doppler signature shown in Fig. 9(b) for this case is very different from the signature of walking with a concealed rifle. As shown in the micro-Doppler signature, arm swings produce large positive and negative frequency shifts during free walk. This is the most significant feature to distinguish if the test

subject is holding any objects, especially heavy things, during walking [25]. Another observation based on the micro-Doppler signature is that the frequency shifts caused by limb motion are symmetric on different direction if arms swing naturally. This could serve as another feature to differentiate walking without holding anything versus other activities.

The echoes with highest power density on range-Doppler signatures correspond to torso moves while the weaker echoes correspond to limb moves.

3) Walking With a Cane for the Blind: In this experiment, subjects mimicked blind people walking toward the radar sensor with a cane. The corresponding experiment result is shown in Fig. 9(c). In this experiment, arm swings were limited due to the use of the cane for direction guidance. The highest frequency shifts on the micro-Doppler signature are produced by tapping the metal tip of the cane on the ground. Base on the observation, micro-Doppler signature for this case is very similar to the signature for walking with a concealed rifle in case (a), except that the moving speed is lower. Thus, only using micro-Doppler analysis is not sufficient for detecting a potential active shooter under this situation.

Fortunately, the range-Doppler signature provides useful information for reliable classification in this case. First, since a blind person tends to walk slowly, the radar echoes have a very low speed as shown in Fig. 9(c). Furthermore, even if a blind person walks fast or a potential shooter intentionally walks slowly, the range-Doppler echoes are still significantly different, as the echoes in Fig. 9(c) occupies much longer range than other cases. This is because the cane always reaches out from the walking person to probe the ground ahead. And the radar sensor detects the walking person and the cane as a whole moving target with a much longer range [25]. On the other hand, a person with a concealed weapon usually occupies a shorter range on range-Doppler signature.

4) Walking With a Gym Bag: The experiment result for this case is shown in Fig. 9(d). In this case, some of the arm swings were limited due to the weight of the gym bag. However, since the subject did not try to keep the gym bag as close as possible to his/her body, there were still some arm swings during the walk. Thus, the micro-Doppler signature of this case is similar to the signature of subject walking without holding anything. Although the frequency shifts caused by arm swing in this case is smaller, the difference between walking with a gym bag and walking with a concealed rifle could be easily identified on the micro-Doppler signatures, as there is no gap between frequency shifts similar to that shown on the micro-Doppler signature of Fig. 9(a) for the rifle's muzzle.

On the other hand, the radar echoes representing the walking person are shown on the range-Doppler frames. They present useful range information to localize the walking person.

5) Walking With a Laptop: In this experiment, the subjects were asked to carry a laptop under his/her arm when he/she walked toward the radar. The purpose of this experiment is to see if the radar is able to differentiate rifle from other large metal objects. A laptop was chosen for this experiment since it is one of the most popular objects carried in our daily life and it has metal parts. The experiment results for this case are shown in Fig. 9(e). The micro-Doppler for this case is similar to the micro-Doppler signature for walking with a gym bag case. This is because the arm swing patterns are similar. Thus, the difference between walking with a laptop and walking with a concealed rifle also could be easily identified on the micro-Doppler signatures.

Similar to other cases, the radar echoes representing the walking person on the range-Doppler frames provide useful range information to localize the walking person.

6) Walking With a Walker: The subjects were asked to walk with a walker in this experiment. Fig. 9(f) shows the experiment results for this case. As shown in the micro-Doppler signature, there is not much negative frequency shift. This is because the metal walker was always moving forward. The strong reflection from the metal structure dominates the signal and produces high power density on the positive Doppler frequency shift side. Thus, the micro-Doppler signature for this case shows a significant difference from the walking with a concealed rifle case.

In the meanwhile, the range-Doppler signatures are able to track the location of the moving person in real time.

7) Moving in a Wheelchair: The subjects were asked to move toward the radar in a wheelchair and the experiment results are shown in Fig. 9(g). The micro-Doppler signature for this case is similar to the case of walking with a walker. Most of the high power density signals appear on the positive Doppler frequency shift side. The reason is also similar to the last case: the metal structure of the wheelchair moved forward and dominated the signal. A few negative frequency shifts are produced with weaker signal strength due to hand movement of the person in the wheelchair.

The location of the moving target is shown on the range-Doppler images in Fig. 9(g).

8) Walking With a Rolling Suitcase: In this experiment, the subjects were asked to walk toward the radar with a rolling suitcase. The result is shown in Fig. 9(h). The metal structure of the suitcase has higher reflection than other moving objects. Thus, the micro-Doppler signature produced in this case has strong signal strength on the positive frequency shifts side. This result is similar to those of experiments *6)* and *7)*.

Similarly, the range-Doppler images contain location information of the moving target.

IV. Feature Extraction and Activity Classification

Feature extraction is very important for getting a high activity classification accuracy. In this work, based on the observation and discussion in section III, four features are extracted from the micro-Doppler signature and one feature is extracted from the range-Doppler signature for activity recognition. Those features are computed from the micro-Doppler and range-Doppler signatures directly. The robustness of the proposed feature extraction algorithm is evaluated under different noise levels. An artificial neural network (ANN) is applied for activity classification. Popular feature selection methods such as the principal component analysis (PCA) and the convolutional neural network (CNN) require one image as one sample to present one activity. In this work, two images (micro-Doppler and range-Doppler) are generated by

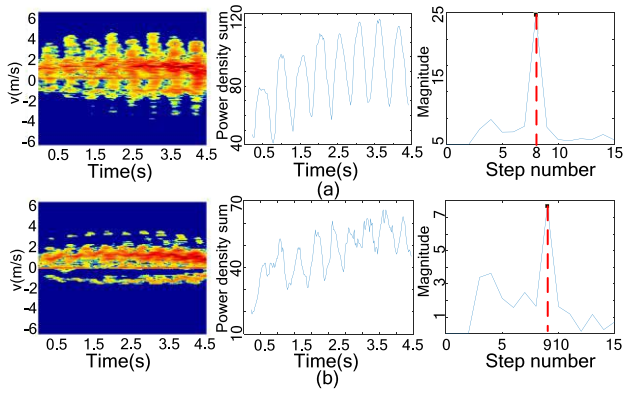

Fig. 10. Examples of step recognition when (a) a human subject walks toward radar sensor without holding anything and (b) a human subject walks toward radar sensor with a concealed rifle.

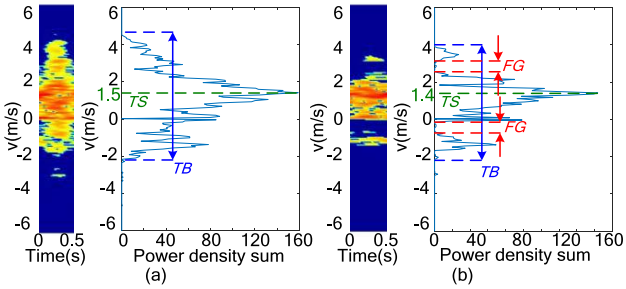

Fig. 11. Feature extraction from micro-Doppler signature when (a) a human subject walks toward radar without holding anything and (b) a human subject walks toward radar with a concealed rifle.

one activity. Thus, the features used in this work are extracted based on the differences of radar signatures between each activity.

In this section, the feature extraction process will be explained in detail. The activity classification using ANN will be introduced and the classification under different noise levels will be studied in this section as well.

A. Features Extracted From Micro-Doppler Signature

Since every single step is treated as one sample during classification process, counting step numbers and recognizing each step from each micro-Doppler signature is necessary. In order to do this, every micro-Doppler signature is processed as a 2-dimensional array and the element of this array is the power density value on the signature. Fig. 10 shows two examples of determining the number of steps and recognizing each step in a micro-Doppler signature. In Fig. 10(a), the figure on the left is a micro-Doppler after noise removal when a human subject walks toward the radar sensor without holding anything. A sum operation of the power density value is applied on velocity direction (y-axis) on the signature and the result is plotted as the middle figure of Fig. 10(a). By doing this, the shape of each step is identified. Then, the local minima are found and processed as the boundaries of different steps. An FFT is applied to the power density sum and the peak of the FFT result corresponds to the number of steps for that micro-Doppler. The right plot of Fig. 10(a) shows the FFT result. It can be seen that this micro-Doppler signature contains eight steps.

Fig. 10(b) is an example of the step counting and recognizing process of a micro-Doppler signature obtained when a human subject walks toward the radar with a concealed rifle. The FFT result shows this micro-Doppler contains nine steps.

It is necessary to mention that the FFT operation is not necessary if the curve of power density sum is smooth (i.e. the middle plot of Fig. 10(a)) and the local minima are easy to identify. However, sometimes, the power density curve is not that smooth (i.e. the middle plot of Fig. 10(b)) and more than one local minima are identified in a small area. In those cases, the FFT operation is needed to recognize the boundary of each step.

After step recognition, the micro-Doppler signature of every single step is treated as one sample. In order to perform feature extraction, a sum operation of power density is taken on the time direction (x-axis). Fig. 11 shows two examples of how features are extracted from the micro-Doppler signature of each step. In each sub-figure, left plot shows the signature of one step and the right one shows the result of the sum operation. Fig. 11(a) corresponds to a step when the human subject walks toward radar without holding anything and Fig. 11(b) is an example when the human subject takes one step toward radar with a concealed rifle. Based on the observation and comparison made in section III, four features are extracted from each sample. The features are defined and calculated as follows:

1) Frequency Gap: As mentioned in section III, when a human subject walks toward the radar sensor with a concealed weapon or a cane for blind, the arm movement is limited and the power density band related to human body movement is narrowed. At the same time, the muzzle of the gun or the metal tip of the cane produce high-energy signature with a high Doppler frequency shift. Thus, a gap is created between the signature of human body movement and that of muzzle/metal tip movement on the micro-Doppler graph. This frequency gap is labeled as *FG* on the power density sum plot of Fig. 11(b). Since there is no frequency gap on the signature in Fig. 11(a), this feature is not labeled in this case.

2) Total Bandwidth: The total bandwidth feature is labeled as *TB* in Fig. 11. It is defined as the difference between the largest positive frequency shift and the lowest negative frequency shift on micro-Doppler signature [3]. The total bandwidth contains information related to human subject's movement amplitude in each step. When a person walks without holding anything, the natural arm swings produce a large total bandwidth. When the human subject walks with a concealed rifle or a cane for blind, the gun's muzzle or the cane's metal tip also produces relatively large total bandwidth.

On the other hand, when the person carries a gym bag or similar objects, the total bandwidth is relatively small due to the limited arm movement.

3) Torso Speed: The torso speed [3] is labeled as *TS* in Fig. 11. Based on the observation of micro-Doppler signatures, torso movements produce the highest power density.

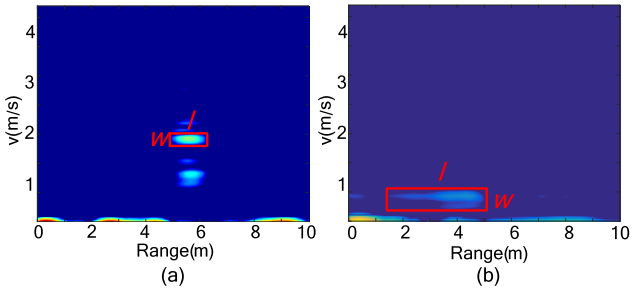

Fig. 12. Feature extraction from range-Doppler signatures when (a) a human subject walks toward radar with a concealed rifle and (b) a human subject walks toward radar with a cane for blind person.

Thus, the torso speed is obtained by finding the velocity corresponding to the highest power density point. As shown Fig. 11, the torso speeds for these two examples are 1.5 m/s and 1.4 m/s, respectively.

A person with a cane for blind tends to walk slowly. Therefore, the value of this feature should be relatively small for the case of walking with a cane. However, sometimes, a potential active shooter may have abnormal behavior and walk slowly. In those cases, the feature extracted from range-Doppler signature could be the most effective feature to differentiate person with and without a concealed rifle. This feature will be introduced in part *B* of this section.

4) Limb Speed Difference on Different Directions: Since the subjects were always asked to walk toward the radar, the limb speed on positive Doppler frequency shift direction is calculated as the largest positive Doppler frequency shift minus the torso speed (TS). The limb speed on negative Doppler frequency shift direction is the lowest negative frequency shift.

The limb speed difference on different directions is defined as the absolute difference between the limb speed on different directions. If a person walks with natural arm swings, the Doppler frequency shift caused by limb motion on both directions should be symmetric. This feature helps to identify if the human subject is carrying anything.

B. Feature Extracted From Micro-Doppler Signature

One feature is extracted from range-Doppler signature and is defined as echo aspect ratio. Fig. 12 shows two examples of how to extract the echo aspect ratio from range-Doppler signatures. In each signature, the area contains the highest power density will be selected as the echo corresponding to human subject's torso. The echo aspect ratio is calculated as the length of the selected echo on the velocity direction (w) divide the length of the same echo on the range direction (l).

As mentioned in section III, the radar sensor recognizes the person with a cane for blind as a single target with a long range. Thus, as labeled in Fig. 12(b), the length of the selected echo on the velocity direction (w) is much smaller than the length along the range direction (l).

C. Activity Classification Using Artificial Neural Network

Table I summarizes the activities studied in this work and the features extracted from micro-Doppler and range-Doppler signatures. A typical value of each feature for different activities is shown in Table II. Each value in this table is obtained by averaging five randomly selected feature values for each activity. It is shown that some of the feature values make certain activity distinguishable from other activities. For example, the walking with a concealed rifle (A-1) and walking with a cane for blind (A-3) have relatively larger frequency gaps (F-1) compared with the other two activities. Walking with a cane for blind (A-3) has a much smaller echo aspect ratio (F-5) than those of other activities.

After extracting features from micro-Doppler and range-Doppler signatures, the artificial neural network (ANN) is adopted for activity classification. The proposed ANN employs a multilayer feedforward network structure with one hidden layer. The inputs of this ANN are five features and the outputs are eight identified activities. Based on the empirical rule-of-thumb, the optimal number of hidden layer neurons is between the size of the input layer and the size

TABLE I
SUMMARY OF ACTIVITIES AND EXTRACTED FEATURES

Activity Notation	Activity Description	Feature Notation	Feature Description
A-1	Walking with a concealed rifle	F-1	Frequency gap
A-2	Walking without holding anything	F-2	Total bandwidth
A-3	Walking with a cane for blind	F-3	Torso speed
A-4	Walking with a gym bag	F-4	Doppler shift difference between two directions
A-5	Walking with a laptop	F-5	Echo aspect ratio
A-6	Walking with a walker		
A-7	Moving in a wheelchair		
A-8	Walking with a rolling suitcase		

TABLE II
TYPICAL VALUE OF EACH FEATURE FOR DIFFERENT ACTIVITIES

	F-1	F-2	F-3	F-4	F-5
A-1	0.335	0.89	1.470	1.511	0.734
A-2	0.134	1.35	1.450	1.022	0.704
A-3	0.420	0.72	1.020	1.411	0.102
A-4	0.161	1.03	1.460	1.346	0.736
A-5	0.152	1.01	1.430	1.532	0.754
A-6	0.025	1.19	1.235	1.425	0.693
A-7	0.054	1.10	1.335	1.442	0.682
A-8	0.102	1.15	1.402	1.522	0.701

TABLE III
NUMBER OF SAMPLES COLLECTED FROM EACH SUBJECT FOR EACH ACTIVITY

Subject\Activity	A-1	A-2	A-3	A-4
Male	425	425	305	310
Female	140	140	105	103
Subject\Activity	A-5	A-6	A-7	A-8
Male	425	425	395	400
Female	135	160	135	130

TABLE IV
CONFUSION MATRIX OF ACTIVITY CLASSIFICATION USING ANN BASED ON THE EXTRACTED FEATURES

Out\Tar*	A-1	A-2	A-3	A-4	A-5	A-6	A-7	A-8
A-1	100%	6.3%	0	0	0	0	0	0
A-2	0	93.7%	0	0	0	0	0	0
A-3	0	0	100%	0	0	0	0	0
A-4	0	0	0	52.1%	33.6%	0	0	0
A-5	0	0	0	47.9%	66.4%	0	0	0
A-6	0	0	0	0	0	32.8%	32.9%	18.5%
A-7	0	0	0	0	0	22.4%	52.1%	33%
A-8	0	0	0	0	0	44.8%	15%	48.5%

*Out represents output class and Tar represents target class.

of the output layer. Thus, the number of neurons of the hidden layer is chosen to be five in this work. The ReLU activation function is used in this study. Gradient descent is adopted as the optimizer. It updates weight and bias value based on an adaptive learning rate. The learning rate in this work is set to be 0.01. Table III shows the number of samples collected from different human subjects for each activity. A total of 4158 samples were collected. Among those 4158 samples, 3085 samples were collected when the movements were parallel (0°) to the antenna's main lobe. 524 samples were collected when the movements were 15° to the radar's main lobe, while 549 samples were collected when there was a 35° angle between the antenna's main lobe and the movements.

In order to test the ANN's classification capability, a training-validating-testing structure is used. 70%, 15%, and 15% of the samples are used for training, validating, and testing, respectively. Table IV shows the confusion matrix for this case.

The classification results related to activity A-1 (walking with a concealed rifle) are highlighted in green in the confusion matrix. The results show that the overall accuracy for differentiating activity A-1 and other similar activities achieved 99.21%. Among those similar activities, 6.3% of the samples from A-2 (walking without anything) are recognized as A-1. Other than this, all the other activities are successfully differentiated from the case of walking with a concealed rifle regardless of the angle between the movements and the radar.

It can be seen from the table that activity A-4 (walking with a gym bag) is confused with activity A-5 (walking with a laptop). This is because the arm swings are similar in these two cases and produced similar micro-Doppler and range-Doppler signatures. The proposed method is not able to recognize activities among A-6 (walking with a walker), A-7 (moving in a wheelchair) and A-8 (walking with a rolling suitcase). This is because large metal objects in those experiments result in similar signatures. However, the purpose of this work is to differentiate activity A-1 (walking with concealed rifle) from other activities and this goal is achieved by the proposed method.

D. Classification Under Different Noise Levels

To evaluate the robustness of the proposed classification algorithm under different noise levels, white Gaussian noises with different signal-to-noise-ratios (SNR) are added to the original signals and the corresponding radar signatures are obtained. Fig. 13 shows an example of the same measured micro-Doppler with different SNR values.

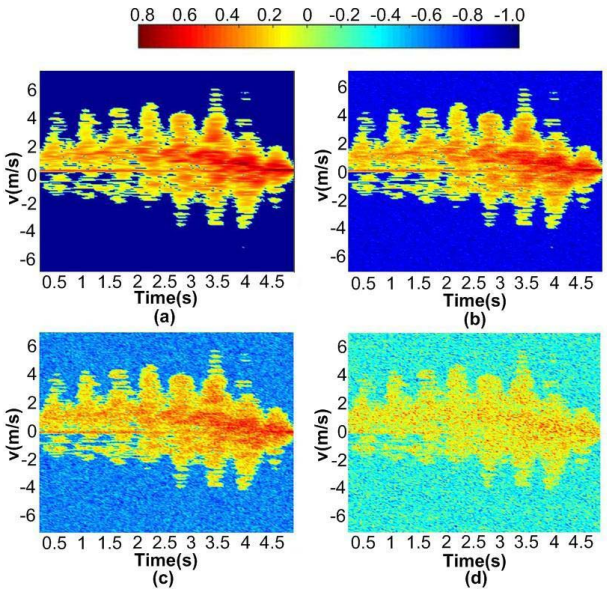

Fig. 13. Micro-Doppler signatures for the same experiment with different levels of additive Gaussian noise: (a) original signal, (b) −10 dB SNR, (c) −20 dB SNR and (d) −30 dB SNR.

TABLE V
CLASSIFICATION RESULTS UNDER DIFFERENT SNR VALUES

SNR (dB)	-10	-20	-30
Classification Result	98.7%	96.7%	86.4%

All the samples from both micro-Doppler and range-Doppler signatures with different SNR values are tested by the proposed classification method. Table V shows the classification results of identifying a subject walking with a concealed rifle from other tested cases under different SNR values. As shown in the table, the classification results achieve accuracies better than 96.7% when the SNR values are above −20 dB. This is because the proposed feature extraction algorithm calculates all the feature values based on the number of pixels. As long as the shape of the movement can be recognized on the signature, the calculated feature values would not change too much under different SNR values.

On the other hand, the recognition result drops dramatically when the SNR value decreases to −30 dB. This is because the

shape of the movement is getting difficult to be recognized when the signatures get unclear. Therefore, it is found that the classification result is reasonable as long as the SNR of the baseband output is above −20 dB.

V. Conclusion

This work investigated the feasibility of using portable radar for micro-Doppler and range-Doppler identification of a potential active shooter who carries a concealed weapon. A custom-designed 5.8-GHz hybrid-mode FMCW-Doppler radar sensor was adopted in this work to carry out the experiment. Thirteen human subjects were used to perform eight activities for multiple times, with different angles to the radar main lobe.

Compared with optical technologies, the proposed solution can sense through clothing while posing less privacy concerns. To evaluate the false alarm rate, seven activities similar to carrying a concealed weapon were also studied. Five features were extracted from the micro-Doppler and range-Doppler signatures. The proposed feature extraction algorithm was examined under different noise levels. An ANN was trained to classify different activities. The classification results showed an average accuracy of 99.21% for differentiating a subject walking with a concealed rifle and other seven similar activities.

This work focused on the specific case of detecting a person walking with a concealed rifle hidden under the trench coat. It should be noted that the main reason for this research was to show that radar sensor could provide an added layer of security with a low cost and minimum interference with normal indoor activities. The radar-based detection method investigated in this paper could be integrated into current shooter detection systems to improve the usability, reliability, and robustness.

References

[1] Federal Bureau of Investigation, *Active Shooter Incidents in the United States in 2014 and 2015*, U.S. Dept. Justice, Washington, DC, USA, Sep. 2013.

[2] T. Smith, "Weapon location by acoustic-optic sensor fusion," U.S. Patent 6621764, Sep. 16, 2003.

[3] Y. Kim and H. Ling, "Human activity classification based on micro-Doppler signatures using a support vector machine," *IEEE Trans. Geosci. Remote Sens.*, vol. 47, no. 5, pp. 1328–1337, May 2009.

[4] Y. Kim and H. Ling, "Human activity classification based on micro-Doppler signatures using an artificial neural network," in *Proc. IEEE Antennas Propag. Soc. Int. Symp.*, Jul. 2008, pp. 1–4.

[5] D. Tahmoush, J. Silvious, and J. Clark, "An UGS radar with micro-Doppler capabilities for wide area persistent surveillance," *Proc. SPIE*, vol. 7669, pp. 766904–766911, Apr. 2010.

[6] L. Du, L. Li, B. Wang, and J. Xiao, "Micro-Doppler feature extraction based on time-frequency spectrogram for ground moving targets classification with low-resolution radar," *IEEE Sensors J.*, vol. 16, no. 10, pp. 3756–3763, May 2016.

[7] L. Du, Y. Ma, B. Wang, and H. Liu, "Noise-robust classification of ground moving targets based on time-frequency feature from micro-Doppler signature," *IEEE Sensors J.*, vol. 14, no. 8, pp. 2672–2682, Aug. 2014.

[8] S. Z. Gurbuz, C. Clemente, A. Balleri, and J. J. Soraghan, "Micro-Doppler-based in-home aided and unaided walking recognition with multiple radar and sonar systems," *IET Radar, Sonar Navigat.*, vol. 11, no. 1, pp. 107–115, Jan. 2017.

[9] J. Hong, S. Tomii, and T. Ohtsuki, "Cooperative fall detection using Doppler radar and array sensor," in *Proc. IEEE PIMRC*, London, U.K., Sep. 2013, pp. 3492–3496.

[10] K. Saho, M. Fujimoto, M. Masugi, and L.-S. Chou, "Gait classification of young adults, elderly non-fallers, and elderly fallers using micro-Doppler radar signals: Simulation study," *IEEE Sensors J.*, vol. 17, no. 8, pp. 2320–2321, Apr. 2017.

[11] Y. Kim and B. Toomajian, "Hand gesture recognition using micro-Doppler signatures with convolutional neural network," *IEEE Access*, vol. 4, pp. 7125–7130, 2016.

[12] Q. Wan, Y. Li, C. Li, and R. Pal, "Gesture recognition for smart home applications using portable radar sensors," in *Proc. 36th Conf. IEEE Eng. Med. Biol. Soc.*, Aug. 2014, pp. 6414–6417.

[13] D. Tahmoush and J. Silvious, "Radar polarimetry for security applications," in *Proc. 7th Eur. Radar Conf.*, Paris, France, Sep./Oct. 2010, pp. 471–474.

[14] F. Fioranelli, M. Ritchie, and H. Griffiths, "Multistatic human micro-Doppler classification of armed/unarmed personnel," *IET Radar, Sonar Navigat.*, vol. 9, no. 7, pp. 857–865, Aug. 2015.

[15] B. Jokanovic, M. Amin, and B. Erol, "Multiple joint-variable domains recognition of human motion," in *Proc. IEEE Radar Conf.*, Seattle, WA, USA, May 2017, pp. 948–952.

[16] B. Jokanović and M. Amin, "Suitability of data representation domains in expressing human motion radar signals," *IEEE Geosci. Remote Sens. Lett.*, vol. 14, no. 12, pp. 2370–2374, Dec. 2017.

[17] B. Jokanović and M. Amin, "Fall detection using deep learning in range-Doppler radars," *IEEE Trans. Aerosp. Electron. Syst.*, vol. 54, no. 1, pp. 180–189, Feb. 2018.

[18] A. Balleri, K. Chetty, and K. Woodbridge, "Classification of personnel targets by acoustic micro-Doppler signatures," *IET Radar, Sonar Navigat.*, vol. 5, no. 9, pp. 943–951, Dec. 2011.

[19] X. Shi, F. Zhou, M. Tao, and Z. Zhang, "Human movements separation based on principle component analysis," *IEEE Sensors J.*, vol. 16, no. 7, pp. 2017–2027, Apr. 2016.

[20] F. Fioranelli, M. Ritchie, and H. Griffiths, "Performance analysis of centroid and SVD features for personnel recognition using multistatic micro-Doppler," *IEEE Geosci. Remote Sens. Lett.*, vol. 13, no. 5, pp. 725–729, May 2016.

[21] F. Ali and M. Vossiek, "Detection of weak moving targets based on 2-D range-Doppler FMCW radar Fourier processing," in *Proc. IEEE German Microw. Conf.*, Mar. 2010, pp. 214–217.

[22] G. Wang, J.-M. Muñoz-Ferreras, C. Gu, C. Li, and R. Gómez-García, "Application of linear-frequency-modulated continuous-wave (LFMCW) radars for tracking of vital signs," *IEEE Trans. Microw. Theory Techn.*, vol. 62, no. 6, pp. 1387–1399, Jun. 2014.

[23] Z. Peng, J.-M. Muñoz-Ferreras, R. Gómez-García, L. Ran, and C. Li, "24-GHz biomedical radar on flexible substrate for ISAR imaging," in *Proc. IEEE Int. Wireless Symp.*, Mar. 2016, pp. 1–4.

[24] Z. Peng *et al.*, "A portable FMCW interferometry radar with programmable low-IF architecture for localization, ISAR imaging, and vital sign tracking," *IEEE Trans. Microw. Theory Techn.*, vol. 65, no. 4, pp. 1334–1344, Apr. 2017.

[25] Y. Li, Z. Peng, and C. Li, "Potential active shooter detection using a portable radar sensor with micro-Doppler and range-Doppler analysis," in *Proc. Int. Appl. Comput. Electromagn. Soc. Symp. (ACES)*, Suzhou, China, Aug. 2017, pp. 1–2.

[26] R. Rytel-Andrianik, P. Samczynski, D. Gromek, M. Wielgo, J. Drozdowicz, and M. Malanowski, "Micro-range, micro-Doppler joint analysis of pedestrian radar echo," in *Proc. IEEE SPSympo*, Jun. 2015, pp. 1–4.

Yiran Li (S'11) received the B.S. degree in electrical engineering from Southern Medical University, China, in 2009, and the M.S. degree in electrical engineering from Texas Tech University in 2012, where she is currently pursuing the Ph.D. degree in electrical engineering.

From 2015 to 2016, she was with Advanced Bionics, Valencia, CA, USA, where she worked on cochlear implant designs. From 2016 to 2017, she served as the CTO of a startup company, yearONE, LLC, Lubbock, TX, USA, where she worked on radar technology-based baby monitor design. In the summer of 2017, she worked as an intern at the United Technologies Research Center, East Hartford, CT, USA, where she was focused on human detection algorithm development using FMCW radar.

Her research interests include radar sensor designs for biomedical and security applications.

Zhengyu Peng (S'15) received the B.S. degree in electrical engineering from Zhejiang University, Hangzhou, China, in 2011, the M.Sc. degree in electrical engineering from Zhejiang University, Hangzhou, in 2014, and the Ph.D. degree in electrical engineering from Texas Tech University, Lubbock, TX, USA, in 2018.

In the summer of 2017, he was with Mitsubishi Electric Research Laboratories, Cambridge, MA, USA, where he was working on a novel deign of a digital beamforming transmitter architecture for radars and MIMO systems. He is currently with Aptiv, Kokomo, IN, USA, as a Senior Radar Systems Engineer. His research interests include automotive radar, antennas, microwave circuits, and biomedical applications of microwave/RF circuits and systems.

Dr. Peng was a recipient of the 2016 IEEE Microwave Theory and Techniques Society (MTT-S) Graduate Fellowship. He received the third place in the Student Design Competition for High Sensitivity Radar in the 2015 IEEE International Microwave Symposium (IMS), and was a recipient of the Excellent Demo Track Presentation Award in the 2016 IEEE Radio & Wireless Week. He has reviewed over 50 journal papers for the IEEE TRANSACTIONS ON MICROWAVE THEORY AND TECHNIQUES, the IEEE TRANSACTIONS ON INSTRUMENTATION AND MEASUREMENT, the IEEE TRANSACTIONS ON CIRCUITS AND SYSTEMS I: Regular Papers, the IEEE TRANSACTIONS ON CIRCUITS AND SYSTEMS II: Express Briefs, the IEEE TRANSACTIONS ON MOBILE COMPUTING, and the IEEE TRANSACTIONS ON BIOMEDICAL ENGINEERING.

Ranadip Pal (S'05–M'07–SM'13) received the B.Tech. degree in electronics and electrical communication engineering from the Indian Institute of Technology, Kharagpur, India, in 2002, and the M.S. and Ph.D. degrees in electrical engineering from Texas University, College Station, TX, USA, in 2004 and 2007, respectively. Since 2007, he has been with Texas Tech University, where he is currently an Associate Professor with the Electrical and Computer Engineering Department. His research areas are genomic signal processing, stochastic modeling and control, machine learning and computational biology. He has authored more than 90 peer reviewed articles, including publications in high impact journals such as *Nature Medicine* and *Cancer Cell* and has authored a book entitled *Predictive Modeling of Drug Sensitivity*. He received the NSF CAREER Award in 2010, the President's Excellence in Teaching Award in 2012, the Whitacre Research Award in 2014, and the Chancellor's Council Distinguished Research Award in 2016.

Changzhi Li (S'06–M'09–SM'13) received the B.S. degree in electrical engineering from Zhejiang University, China, in 2004, and the Ph.D. degree in electrical engineering from the University of Florida, Gainesville, FL, USA, in 2009.

In the summers of 2007–2009, he was with Alereon Inc., Ausitn, TX, USA. Then, he was with Coherent Logix Inc., Austin, TX, USA, where he was involved with the ultrawideband (UWB) transceivers and software-defined radio, respectively. He joined Texas Tech University as an Assistant Professor in 2009, and became an Associate Professor in 2014. His research interests include biomedical applications of microwave technology, wireless sensors, and RF/analog circuits.

Dr. Li was a recipient of the IEEE Microwave Theory and Techniques Society (MTT-S) Outstanding Young Engineer Award, the IEEE Sensors Council Early Career Technical Achievement Award, the ASEE Frederick Emmons Terman Award, the IEEE-HKN Outstanding Young Professional Award, the NSF Faculty Early CAREER Award, and the IEEE MTT-S Graduate Fellowship Award. He served as the TPC Co-Chair for the IEEE MTT-S International Microwave Biomedical Conference in 2018 and the IEEE Wireless and Microwave Technology Conference from 2012 to 2013. He is an Associate Editor of the IEEE TRANSACTIONS ON CIRCUITS AND SYSTEMS I and the IEEE JOURNAL OF ELECTROMAGNETICS, RF AND MICROWAVES IN MEDICINE AND BIOLOGY. He served as an Associate Editor for the IEEE TRANSACTIONS ON CIRCUITS AND SYSTEMS II from 2014 to 2015.